Crack–void interaction in polycrystalline alumina

D. R. BISWAS*
Institute of Gas Technology, 3424 South State Street, IIT Center, Chicago, IL 60616, USA

Strength of alumina-void samples have been measured in a four-point bend test. Knoop microhardness indentor was used to introduce controlled surface cracks in sintered alumina containing up to 8 vol % spherical voids for the bend test. It was found that as the volume per cent of voids are increased, the strength remained unchanged as the indented crack interacts with the voids. When strong inclusions are considered, an analysis showed that with increase in volume fraction and decrease in inclusion size, the crack interaction resistance for alumina can be improved significantly.

1. Introduction

When a crack front interacts with an array of second-phase inclusions, it bends to an angle before it moves further. If the inclusions are very weak (e.g. voids or pores), the crack front remains relatively straight and as it interacts with the voids, its velocity changes and a catastrophic failure can be avoided. But, if the inclusions are very strong (e.g. hard particles with good bonding with the matrix), the crack front usually bows between inclusions and moves deeply along the path of easy movement. This results in a higher resistance to crack propagation. Several studies [1–3] indicate that improvement in strength and fracture toughness for a two-phase composite are primarily due to a line-tension effect at the crack front.

In the present investigation, an experimental result is presented using a model polycrystalline alumina ceramic containing spherical voids (as weak inclusions) of uniform size and the interaction of a surface crack (produced by Knoop microhardness indentor [4–6] with the voids). Also reported, a simple analysis of the effect of volume fraction and inclusion size on the resistance of crack interaction, when a crack front interacts with the stronger inclusions in polycrystalline alumina (for an example).

2. Experimental procedure

Alumina powder was prepared by mixing Linde A alumina with 0.1 wt % MgO [as $Mg(NO_3)_2 \cdot 6H_2O$] and 2 wt % polyvinyl alcohol (as a binder) with isopropyl alcohol in a Sweco† vibratory energy mill for 2 h using alumina balls. The slurry was dried and passed through − 325 mesh screen. An organic spherical powder was used to produce artificial voids into alumina matrix. Controlled amounts of alumina powders were dry mixed thoroughly with different volume fraction of organic powders (after size separation) and cold pressed into pellets using $13.8\,MN\,m^{-2}$ pressure. These pellets were isostatically pressed at $172.4\,MN\,m^{-2}$ by the wet-bag method. The green density of the pellets was nearly 45% of the theoretical density. The pellets were fired at $800°\,C$ for 4 h to remove the organic content and the binder and to decompose the magnesium nitrate to oxide. The pellets were then sintered at $1750°\,C$ for 1 h in a molybdenum furnace under a high vacuum ($\sim 10^{-6}$ torr). After sintering, the densities of the samples were measured by the Archimedes principle and also from their dimensions and weights. The pellets were cut into strength specimens with a diamond saw. Rectangular bars (26 mm × 2.6 mm × 1.3 mm) were indented by the microhardness indentor which
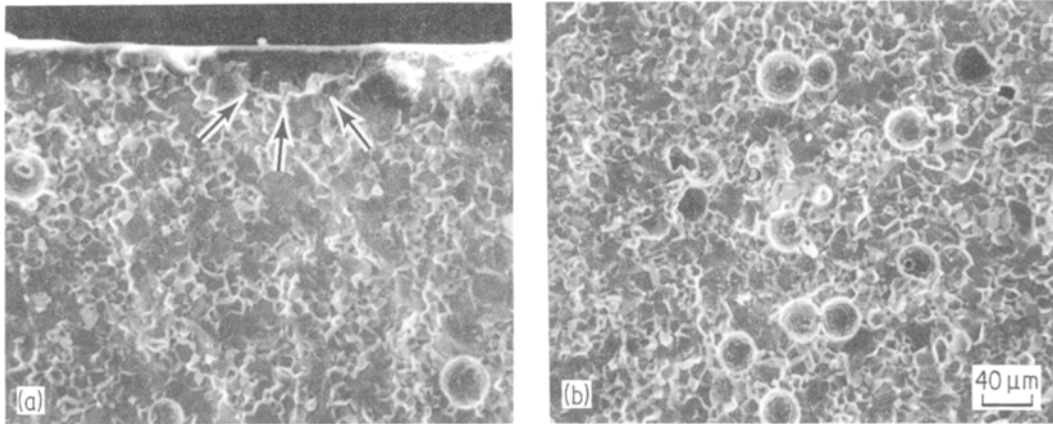
Figure 1 (a) SEM micrograph of $Al_2O_3-2\,vol\%$ voids sample indented at $1000\,g$ load showing a semicircular crack, (b) typical fracture surface of $Al_2O_3-5\,vol\%$ voids sample.

produced a semicircular crack. The indentation load was varied from 500 to 2500 g. Strength of indented specimens was measured at room-temperature in a four-point bend jig with an outer and inner span of 19 and 6 mm, respectively. A cross-head speed of $0.254\,mm\,min^{-1}$ was used. The crack depth was measured from the fractured specimens using optical and scanning electron microscopy (SEM).

3. Results

Fig. 1a is a SEM micrograph showing a semi-circular crack with voids in an alumina specimen. Fig. 1b shows a typical distribution of spherical voids (around $40\,\mu m$ in diameter) in an alumina matrix. A microstructure [7] of polished and thermally etched ($1400°\,C$ in air for 4 h) section of a similar alumina sample (Fig. 2) showing few pores ($\sim 2\,\mu m$) at the grain boundaries and a few
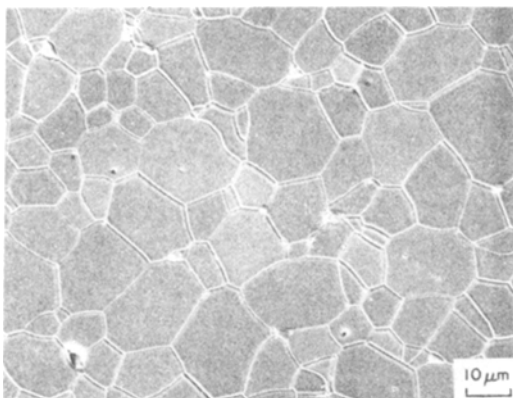
Figure 2 A random selection of polished and thermally etched dense alumina specimen [7].

pores ($1\,\mu m$) inside the alumina grains. A combination of intergranular and transgranular fracture of alumina were observed. Fig. 3 shows a plot of strength against the indentation load. In dense alumina, the strength remains unchanged up to 500 g and then drops with an increase in inden-tation load. But it is quite interesting to note that for 5 and 8 vol% voids, the strength remains un-changed with slight increase with increase in indentation load. Also in Fig. 3, the crack depth is shown to follow a linear increase with increase in indentation load. Fig. 4 shows the strength drop with increase in volume per cent of voids.

4. Discussion

As reported in an earlier paper [3] that the stress (σ_c) necessary to propagate a pre-existing crack through a series of inclusions was given by Lange [1] using Griffith's [8] equation as

$$\sigma_c = \left[\frac{2E}{\pi a}\left(\gamma_m + \frac{T}{d}\right)\right]^{1/2} \qquad (1)$$

where E is the elastic modulus, γ_m is the fracture surface energy of the matrix, a is the crack depth, T is the line tension energy ($= 2/3\,\gamma a$) of the crack front and d is the effective inclusion spacing.

When a crack front interacts with one of the array of inclusions (Fig. 5), it bends to some angle $0 \leqslant \theta \leqslant \pi$ before it moves further. Considering two types of inclusions: (1) very weak (e.g. voids or pores) and (2) very strong (e.g. solid particles with good interfacial bonding) which interacts with the crack front. If weak inclusions are con-sidered ($\theta \sim \pi$), the crack front remains relatively straight and cuts through (but the velocity of
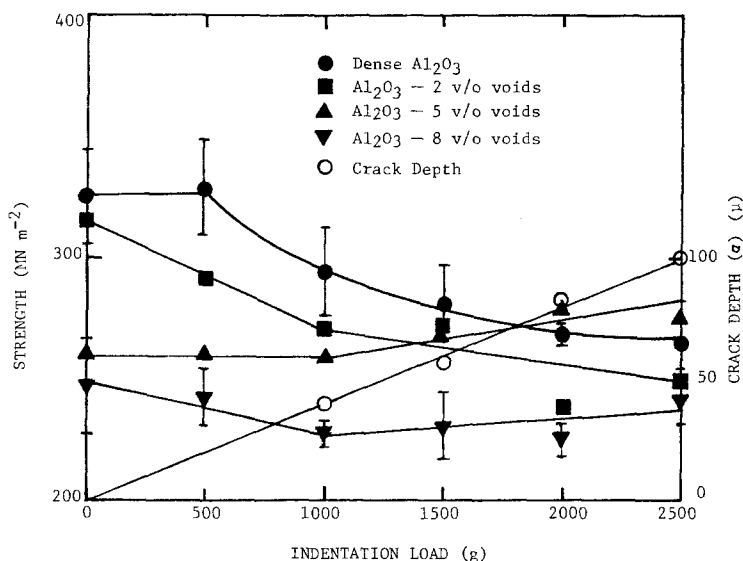
Figure 3 Strength of alumina and alumina–void samples and indentation crack depth plotted against the indentation load.

crack propagation changes when it moves with a velocity of sound. As the sound wave reaches a boundary (e.g. void–matrix interface), the wave will partly be reflected and partly transmitted). The force (F) acting on the inclusions (similarly in case of dislocation interacting with precipitates) was given [9] by

$$F = 2T \cos\left(\frac{\theta}{2}\right). \qquad (2)$$

As the angle θ approaches its critical value θ_c, it breaks away and the corresponding stress (σ) is given by

$$\sigma = 2T/A \cos(\theta/2) \qquad (3)$$

where A is the cross-sectional area created by the new crack surfaces.

In an alumina–void system, when the semi-circular crack* interacts with an array of voids, the velocity of crack propagation checks temporarily and the strength remains unchanged as evidenced from Fig. 2 (particularly in the case of 5 and 8 vol % voids). But, the situation will
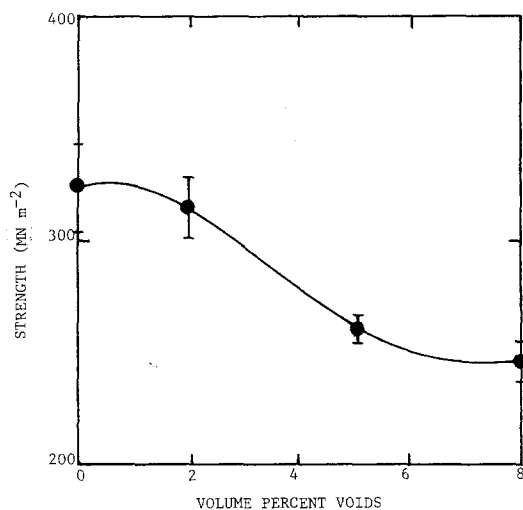
Figure 4 Strength of alumina decreasing in presence of voids.
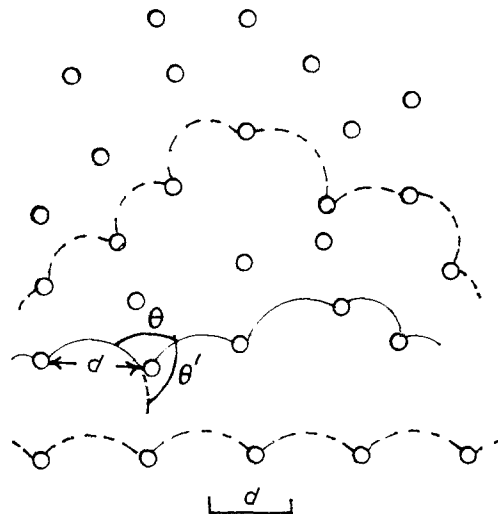
Figure 5 A crack front interacting with weak inclusions. It remains relatively straight and cuts through.

*With regard to using indentation fracture modes for introducing surface cracks, it has already been reported [4, 10] that local plastic deformation occurs when the indentor produces a permanent impression in the sample. The residual stresses resulting from this indentation can be reduced by heat treatment but the exact determination [4] of the magnitude of the residual stresses is difficult to obtain.
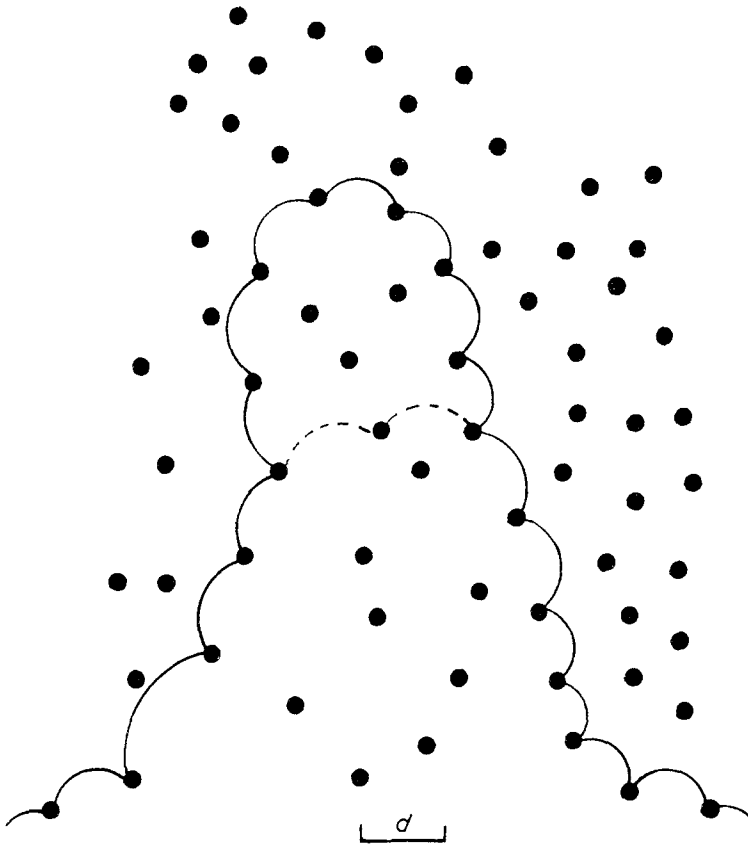
Figure 6 A crack front interacting with strong inclusions. It bows out between inclusions and penetrates the array deeply along the path of easy movement.

be quite different when solid inclusions are considered.

If the inclusions are strong ($\theta \simeq 0$), the crack interacts and frequently penetrates the array deeply along the path of easy movement (Fig. 6). For spherical inclusions with radius, r, the inter-inclusion spacing (d) was calculated [9] as

$$d = [(\pi/f)^{1/2} - 2](2/3)^{1/2} r \qquad (4)$$

where f is the volume fraction of inclusions. Substituting d and T into Equation 1, the stress necessary for crack propagation in a composite (σ_c) is

$$\sigma_c = \left(\frac{2E\gamma_m}{\pi a}\right)^{1/2} \left\{1 + \frac{(2/3)^{1/2} a}{[(\pi/f)^{1/2} - 2] r}\right\}^{1/2}. \quad (5)$$

The first term in Equation 5 can be referred to as the strength of the matrix (σ_m) and the second term is due to the contribution of line tension energy of the crack front and interinclusion spacing. Therefore,

$$\sigma_c = \sigma_m \left\{1 + \frac{(2/3)^{1/2} a}{[(\pi/f)^{1/2} - 2] r}\right\}^{1/2} \quad (6)$$

$$\frac{\sigma_c}{\sigma_m} = \left\{1 + \frac{(2/3)^{1/2} a}{[(\pi/f)^{1/2} - 2] r}\right\}^{1/2}. \quad (7)$$

The ratio σ_c/σ_m can be referred to as the resistance to crack interaction with the inclusions. From Equation 7, a series of curves can be generated by varying f, keeping a and r constant, and also, by varying the size of the inclusions keeping a and f constant. In alumina polycrystalline ceramic, if the inclusions are solid particles with matching thermal expansion (to avoid internal stresses) and good interfacial bonding, two curves can be shown as in Fig. 7 with varying volume fraction of inclusions and inclusion size assuming the critical flaw size in alumina [11] is $\simeq 60\,\mu\mathrm{m}$. Fig. 7 indicates that with increase in volume fraction (i.e. reducing interinclusion distance) and decrease in inclusion size, the crack interaction resistance (σ_c/σ_m) can be improved significantly. This simple analysis can also be used to determine what fraction and inclusion size are needed to achieve a desirable crack interaction resistance if the critical flaw size of the material is known.
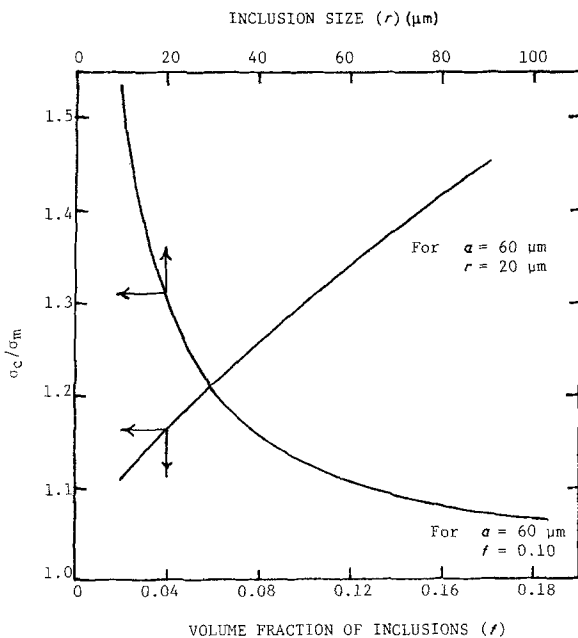
INCLUSION SIZE (r) (μm)

Figure 7 Crack interaction parameter σ_c/σ_m in polycrystalline alumina plotted against the volume fraction of inclusions keeping critical flaw size (a) and radius of inclusion (r) constant. σ_c/σ_m is also plotted against inclusion size keeping the critical flaw size and volume fraction of inclusion constant.

5. Summary and conclusion

In alumina, the strength remains unchanged up to 500 g and then decreases with increase in indentation load. The strength remains unchanged with increase in indentation load in the presence of 5 and 8 vol% spherical voids as the voids act as crack arrestors. When the inclusions are very strong, the crack interaction resistance for alumina can be improved significantly with increase in volume fraction of inclusions and decrease in inclusion size.

Acknowledgement

References

1. F. F. LANGE, *Phil. Mag.* **22** (1970) 983.
2. A. G. EVANS, *ibid.* **26** (1972) 1327.
3. D. R. BISWAS, *J. Mater. Sci.* **15** (1980) 1696.
4. J. J. PETROVIC, L. A. SIMPSON, P. K. TALTY and A. K. VASUDEVAN, *J. Amer. Ceram. Soc.* **58** (1975) 113.
5. B. R. LAWN and R. R. FULLER, *J. Mater. Sci.* **10** (1975) 2016.
6. R. K. GOVILA, K. R. KINSMAN and P. BEARD-MORE, *ibid.* **13** (1978) 2081.
7. J. S. WALLACE, MSc thesis, University of California, Berkeley (1978).
8. A. GRIFFITH, *Phil. Trans. Roy. Soc. (London)* **A221** (1920) 163.
9. L. M. BROWN and R. K. HAM in "Strengthening Methods in Crystals", edited by A. Kelley and R. B. Nicholson (Applied Science Publisher Ltd., London, 1971) p. 9.
10. B. R. LAWN, E. R. FULLER and J. M. WIEDER-HORN, *J. Amer. Ceram. Soc.* **59** (1976) 193.
11. S. W. FREIMAN, K. R. McKINNEY and H. L. SMITH in "Fracture Mechanics of Ceramics", edited by R. C. Bradt, D. P. H. Hasselman and F. F. Lange (Plenum Press, New York and London, 1974) p. 659.